

CALIBRATION OF SIMULATION PARAMETERS OF COATED PARTICLES AND ANALYSIS OF EXPERIMENTAL RESULTS

/

包衣颗粒的模拟参数标定与试验结果分析

Xuejie MA, Zhanfeng HOU*, Min LIU

Inner Mongolia Agricultural University, College of Mechanical and Electrical Engineering, Inner Mongolia, China

Tel: +86 04714309215; *Corresponding author E-mail: njauhzf@163.com

DOI: <https://doi.org/10.35633/inmateh-67-23>

Keywords: Discrete elements; Alfalfa seeds; Coating powder; Calibration of contact parameters

ABSTRACT

Calibrating the contact parameters when carrying out the seed pelletizing coating test could improve the simulation tests' accuracy. In this paper, alfalfa seeds and coated powders (hereafter referred to as seeds and powders) are used as the main object of study to calibrate their contact parameters, using the Hertz-Mindlin no-slip model and the JKR model to calibrate the contact parameters between seeds, between seed and steel plates (coating pot materials), between powder materials, between powder and steel plates, based on EDEM using the angle of repose as the response value to perform the Plackett-Burman test, the steepest ascent experiment, and the Box-Behnken test in turn to obtain the best combination of particle contact parameters, finally conducting physical angle of repose tests for comparison; when calibrating the contact parameters of seed and powder, the physical examinations and the simulation tests are combined to obtain the contact parameters through quadratic regression fitting equations. The difference between the contact parameter combinations obtained from the simulation tests and the physical test results is less than 1%, which provides some reference for calibrating similar fine seeds and powder parameters.

摘要

标定种子进行丸化包衣试验时的接触参数，可提高仿真试验的准确度。本文以紫花苜蓿种子和包衣粉料（以下简称种子和粉料）为主要研究对象标定其接触参数，接触模型分别采用 Hertz-Mindlin 无滑移模型和 JKR 模型（即 Hertz-Mindlin with JKR 模型）标定种子间、种子钢板（包衣锅材料）间、粉料间、粉料钢板间的接触参数，以颗粒休止角为响应值，基于 EDEM 依次开展 Plackett-Burman 试验、最陡爬坡试验以及 Box-Behnken 试验，得到颗粒最佳接触参数组合，最后开展物理休止角试验进行对比；将物理试验与仿真试验相结合标定种子与粉料间的接触参数时，通过二次回归拟合方程得到其接触参数。仿真试验得到接触参数组合与物理试验结果相差均小于 1%，为相似小粒种子及粉料参数标定提供一定参考。

INTRODUCTION

Seed pelletizing is a processing technology that uses seeds as a carrier, uses coating equipment to mix seeds, seed coating agents, coating powders and additives with other active ingredients in a particular ratio and evenly wrap them on the surface of the seeds, which improves the viability and germination rate of the seeds and ensures the integrity of the seeds in the delivery system to realize the automation of agricultural machinery (Afzal, 2020). In the process of seed pellet coating, the collision and extrusion relationships of seed particles, of coated powder particles, of seed particles and powder particles are very complex (Zeng, 2021); discrete element method analysis is helpful to reveal the seed pellet coating mechanism, mixing mechanism and movement law (Gui, 2018).

Domestic and foreign scholars have conducted much research based on the discrete element method. Liu, (2016), compared physical and simulation tests using wheat rest angle as the response value to obtain discrete meta-simulation working parameters for wheat seeds. Horabik, (2017), studied the measurement of the collision recovery coefficient of the same seed at different humidity levels utilizing a high-speed camera. Zhang, (2020), calibrated the working simulation parameters of blueberry based on response surface optimization.

Wu, (2017), used the JKR model to calibrate the sample soil considering the bonding force between particles. Shi, (2017), integrated the delayed elasticity model and the linear cohesion model to establish the soil model in the northwest arid area and calibrate the contact parameters. Ren, (2017), scaled up the cast iron coal powder particles to 2 mm based on similar theory and calibrated the scale-up particles' contact parameters by virtual experiments. This research proposes a method to calibrate the contact parameters between granular and powder materials and analyses the test results. Based on the theory of particle scaling, the contact parameters between seeds, powders, and powders and seeds are calibrated to provide a reference to the discrete element simulation parameter calibration of similar fine particles and powders materials.

MATERIALS AND METHODS

Test material and physical parameter determination

The test materials are the powder made by soybean meal and diatomaceous earth prepared 1:1 and alfalfa seeds. The shear modulus and Poisson's ratio are vital parameters needed for the simulation test, and the seed and powder shear modulus is obtained from Eq.1. The modulus of elasticity of the powder is 7.78×10^7 ; the modulus of elasticity of the seeds is obtained by compression tests with a mass spectrometer (model: TMS-PRO), as shown in Figure 1. Seed Poisson's ratio range is 0.3~0.5, the Poisson's ratio of powder is 0.296 obtained by the fast shear test (Zhao, 2015).

$$G = \frac{E}{2(1+\mu)} \quad (1)$$

Where G is the shear modulus, Pa; E is the elastic modulus, Pa; μ is the Poisson's ratio.

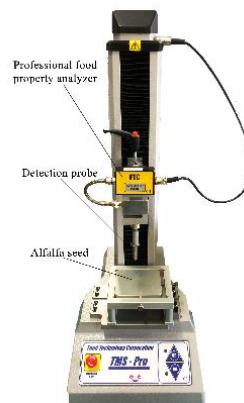


Fig. 1 - Professional food physical property analyser

Contact parameter determination

The collision recovery coefficient reflects the ability of the seed to recover deformation after a collision and is defined as the ratio of the normal separation velocity of the seed after a collision to the normal approach velocity before collision (Liu, 2018). The collision recovery coefficient is measured through the impact bounce test, and the PCO.dimax high-speed camera is used to collect the seed rebound height image, obtaining the collision recovery coefficient between seeds 0.19, between seeds and steel plates 0.5. The test of the collision recovery coefficient of seed and powder is the same as above.

The coefficients of friction are determined by the incline method (Hou, 2020), as shown in Figure 2, the obtained coefficient of static friction between seeds is 0.67, the coefficient of static friction of seeds and steel plates is 0.3; the rolling friction coefficient between seeds is 0.8, the rolling friction coefficient of seeds and steel plates is 0.38. The test for the friction coefficient of seed and powder is the same as above.

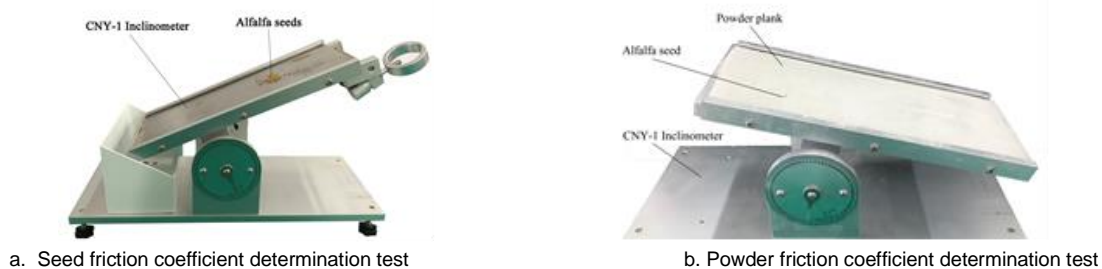


Fig. 2 - Friction coefficient measurement test

The angle of the repose test

The average angle of repose of seeds is 32.74°, the average angle of repose of powders is 41.69° after 10 repeated tests using the FT-104B rest angle tester (Figure 3).

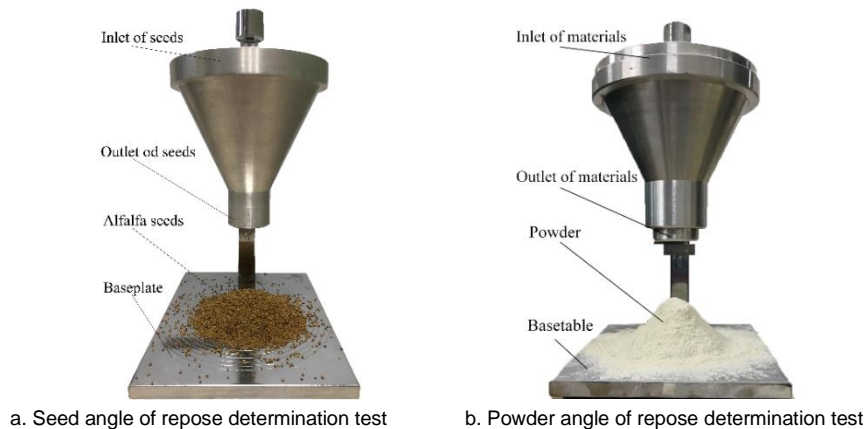


Fig. 3 - The angle of repose determination test

DEM contact model

When the discrete element method is used for the seed simulation test, the Hertz-Mindlin (no-slip) model is adopted; considering that the powder material will unite and agglomerate, the JKR model is used when conducting the powder material simulation test. The JKR model introduces the effect of surface energy on the interaction between particles, which uses the JKR normal elastic contact force F_{JKR} to calculate (Pachón-Morales, 2019), as shown in Eqs.2 and 3.

$$F_{JKR} = -4\sqrt{\pi\gamma E^*} \alpha^{\frac{3}{2}} + \frac{4E^*}{3R^*} \alpha^3 \tag{2}$$

$$\delta = \frac{\alpha^2}{R^*} - \sqrt{\frac{4\pi\gamma\alpha}{E^*}} \tag{3}$$

where: F_{JKR} is the normal elastic force of JKR, N; δ is the normal overlap between two contact particles, m; α is the tangential overlap between two contact particles, m; γ is the surface energy, N/m; E^* is the equivalent elastic modulus, Pa; R^* is the equivalent contact radius, m.

The equivalent elastic modulus E^* and the equivalent contact radius R^* are defined as Eqs.4 and 5.

$$\frac{1}{E} = \frac{1-\nu^2}{E_1} + \frac{1-\nu^2}{E_2} \tag{4}$$

$$\frac{1}{R^*} = \frac{1}{R_1} + \frac{1}{R_2} \tag{5}$$

where: E_1 and E_2 are the elastic modulus of the two contacting particles, Pa; ν_1 and ν_2 are the Poisson's ratio of the two contacting particles; R_1 and R_2 are the contact radii of the two contacting particles, m.

Simulation model establishment

The positions of each sphere of particles composed of multi-spheres are fixed close to the actual shape of seeds, and the simulation accuracy can be improved (Favier, 2001). When using the multi-sphere method, it is crucial to accurately find the balance between the accuracy of the particles and the operating efficiency of EDEM. Markauskas et al., (2015), found that reducing the number of sub-spheres in the corn kernel model successfully simulates corn's unloading in the silo material test. Based on the results of the physical experiment and simulation, taking into account the accuracy and efficiency of the experiment, seven sub-spheres are used to establish a seed model, and the powder particles are a single-sphere model, as shown in figure 4.

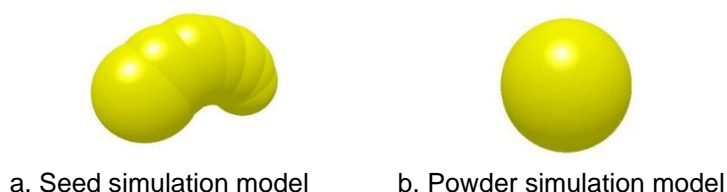


Fig. 4 - Discrete element simulation model

Simulation model establishment

Parameter calibration requires plenty of simulations, and it takes much time to simulate the actual number and size of particles in batch testing; it is laborious to perform many simulations in a real-time frame. After establishing a balance equation between the particle zoom factor and the simulation time, the large particle model is used to conduct the simulation experiment of the material in a short time. Van der Waals force is the primary source of the adhesion of fine particles. In the discrete element modelling of fine particles, the theoretical adhesive elastic model is generally used to express the van der Waals force. *Subhash, (2016)*, gave the relationship about the tensile strength of a rigid monodisperse sphere system and random isotropic materials and the contact force between particles, and its expression is Eq.6.

$$f = \frac{4\pi R^2}{\varphi k_1} \sigma \tag{6}$$

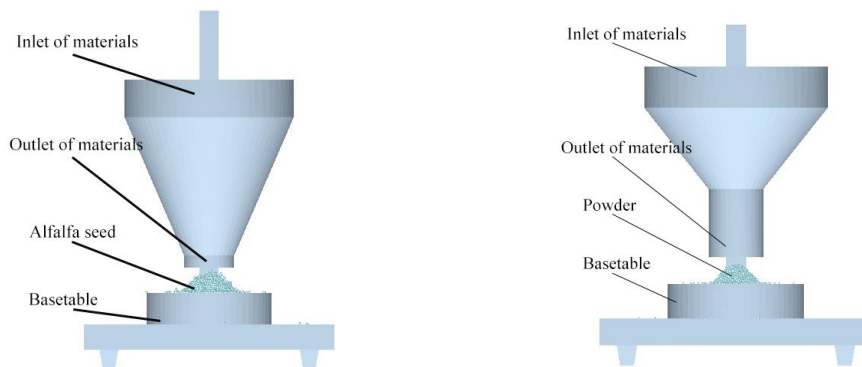
where: f is the contact force between particles, N; φ filling rate, %; k_1 is the coordination number; σ is the tensile strength, MPa.

The formula shows the proportional relationship between the adhesion force and the quadratic of the particle radius. The JKR surface energy of particles changes with the scaling ratio, and it will be calibrated in the follow-up virtual test. Keeping the density constant for scaling the particles, their elastic modulus changes with the scaling of the radius, the larger value being selected according to the range of parameters. In order to ensure the simulation accuracy and work efficiency, this paper enlarges the particles by 6 times for the simulation test (*Zhou, 2017*).

RESULTS AND DISCUSSION

The angle of repose simulation test

EDEM is used to perform the angle of repose simulation test to calibrate the contact parameters of seeds, of seeds and steel plates, of powder materials, of powder materials and steel plates. The model is shown in Figure 5 and the simulation test parameters of seeds and powder are shown in Table 1.



a. Seed angle of repose simulation test b. Powder angle of repose simulation test

Fig. 5 - The angle of repose simulation test

Table 1

Simulation test parameters range

Range of seed simulation test parameters			Range of powder simulation test parameters		
Simulation parameters	Low level	High level	Simulation parameters	Low level	High level
Poisson's ratio A_m	0.3	0.5	Inter-powder collision recovery coefficient A_s	0.05	0.25
Shear modulus B_m	5	15	Inter-powder static friction coefficient B_s	0.7	0.9
Inter-seed collision recovery coefficient C_m	0.1	0.3	Inter-powder rolling friction coefficient C_s	0.25	0.45
Inter-seed static friction coefficient D_m	0.5	0.9	Collision recovery coefficient between powder and steel plate D_s	0.05	0.25
Inter-seed rolling friction coefficient E_m	0.7	0.9	The static friction coefficient between powder and steel plate E_s	0.62	0.82
Collision recovery coefficient between seed and steel plate F_m	0.4	0.6	Rolling friction coefficient between powder and steel plate F_s	0.19	0.39

The static friction coefficient between seed and steel plate G_m	0.25	0.45	JKR surface energy G_s	0.1	0.3
Rolling friction coefficient between seed and steel plate H_m	0.3	0.5		0.05	0.25

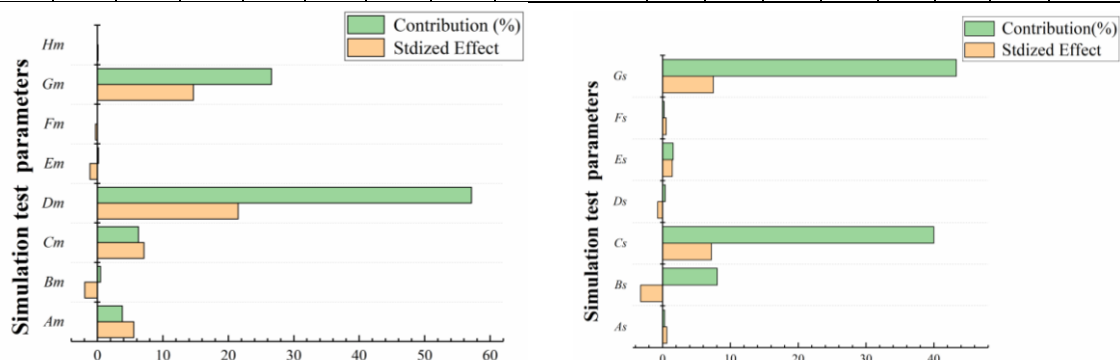
Plackett-Burman test

Use Design-Expert software to conduct Plackett-Burman experiment design, take the angle of repose as the response value, screen out the parameters that significantly influence the response value; the experimental design and results are shown in Table 2.

Table 2

Plackett-Burman test parameters

No.	Seed Plackett-Burman test parameters									Powder Plackett-Burman test parameters							
	A_m	B_m	C_m	D_m	E_m	F_m	G_m	H_m	Angle of repose (°)	A_s	B_s	C_s	D_s	E_s	F_s	G_s	Angle of repose (°)
1	1	1	-1	1	1	1	-1	-1	29.87	1	1	-1	1	1	1	-1	30.86
2	-1	1	1	-1	1	1	1	-1	24.58	-1	1	1	-1	1	1	1	48.00
3	1	-1	1	1	-1	1	1	1	54.84	1	-1	1	1	-1	1	1	49.16
4	-1	1	-1	1	1	-1	1	1	36.31	-1	1	-1	1	1	-1	1	39.11
5	-1	-1	1	-1	1	1	-1	1	8.9	-1	-1	1	-1	1	1	-1	42.73
6	-1	-1	-1	1	-1	1	1	-1	38.94	-1	-1	-1	1	-1	1	1	41.45
7	1	-1	-1	-1	1	-1	1	1	25.31	1	-1	-1	-1	1	-1	1	44.82
8	1	1	-1	-1	-1	1	-1	1	6.52	1	1	-1	-1	-1	1	-1	33.91
9	1	1	1	-1	-1	-1	1	-1	28.48	1	1	1	-1	-1	-1	1	44.41
10	-1	1	1	1	-1	-1	-1	1	32.92	-1	1	1	1	-1	-1	-1	38.53
11	1	-1	1	1	1	-1	-1	-1	36.09	1	-1	1	1	1	-1	-1	43.24
12	-1	-1	-1	-1	-1	-1	-1	-1	6.19	-1	-1	-1	-1	-1	-1	-1	32.78
13	0	0	0	0	0	0	0	0	38.2	0	0	0	0	0	0	0	43.74



a. Analysis of the contribution of seed test results b. Analysis of the contribution of powder test results

Fig. 6 - Analysis of the contribution of Plackett-Burman test results

Table 3

Significance analysis of Plackett-Burman test results

Significance analysis of seed Plackett-Burman test results				Significance analysis of powder Plackett-Burman test results			
Parameters	Degree of freedom	sum of squares	P-value	Parameters	Degree of freedom	sum of squares	P-value
A_m	1	92.24	0.0525	A_s	1	1.20	0.6084
B_m	1	11.19	0.3567	B_s	1	31.23	0.0474*
C_m	1	151.73	0.0280*	C_s	1	155.09	0.0032**
D_m	1	1386.54	0.0012**	D_s	1	1.54	0.5640
E_m	1	3.89	0.5675	E_s	1	6.05	0.2812
F_m	1	0.2269	0.8869	F_s	1	0.86	0.6626
G_m	1	644.89	0.0037**	G_s	1	168.00	0.0028**
H_m	1	0.0352	0.9552				

Note: ** indicates an extremely significant effect ($p < 0.01$), * indicates a significant effect ($p < 0.05$). Same as below

We get the effect of each parameter on the angle of repose and its contribution rate through Figure 7. The standardization effect is positively correlated with the angle of repose in the case of positive values and negatively correlated with the angle of repose in the case of negative values (Peng,2020). From Figure 7 and Table 3, it can be seen that the parameter with the enormous contribution rate has the most significant impact on the angle of repose; the three parameters that have the most significant impact on the seed angle of repose are C_m , D_m , G_m . The three parameters that have the most significant influence on the angle of repose of the powder are B_s , C_s , and G_s .

Steepest ascent experiment

The steepest ascent experiment is designed based on the results of the Plackett-Burman test for the three significant parameters, as shown in Table 4. The seeds have the slightest relative error of the angle of repose at the test level of No. 4, so in the subsequent experiments, the parameters of the No. 4 test are used as the centre point, and the No. 3 and No. 5 are respectively used as low and high levels for experimental design. The powder has the slightest relative error of the angle of repose under test level 2, the test design in the subsequent test, takes test level 2 as the centre point, and the level 1 and level 3 are the low and high levels.

Table 4

Steepest ascent experiment design scheme and results

No.	Seed steepest ascent experiment design and results				Powder steepest ascent experiment design and results			
	C_m	D_m	G_m	Relative Error (%)	B_s	C_s	G_s	Relative Error (%)
1	0.1	0.5	0.25	82.62	0.9	0.25	0.1	22.91
2	0.14	0.58	0.29	51.62	0.86	0.29	0.14	0.50
3	0.18	0.66	0.33	22.33	0.82	0.33	0.18	2.64
4	0.22	0.74	0.37	21.93	0.78	0.37	0.22	4.41
5	0.26	0.82	0.41	29.90	0.74	0.41	0.26	6.86
6	0.3	0.9	0.45	34.24	0.7	0.45	0.30	31.66

Box-Behnken test

Based on the steepest ascent experiment results, the Box-Behnken test with the test parameter levels shown in Table 5 was conducted; the test design scheme and results are shown in Table 6, and the test results analysis is shown in Table 7. The second-order regression equation of the relative error of seeds rest angle and powder rest angle are obtained by multiple regression analysis of the experimental data using Design-Expert 11.0 software, Eq.7 is the second-order regression equation for seeds, Eq.8 is the second-order regression equation for powder.

Parameter level code table

Table 5

Level	Seed test parameters			Powder test parameters		
	C_m	D_m	G_m	B_s	C_s	G_s
-1	0.18	0.66	0.33	0.9	0.25	0.1
0	0.22	0.74	0.37	0.86	0.29	0.14
+1	0.26	0.82	0.41	0.82	0.33	0.18

Box-Behnken experimental design and results

Table 6

No.	Seed test design and results				Powder test design and results			
	C_m	D_m	G_m	Angle of repose (°)	B_s	C_s	G_s	Angle of repose (°)
1	-1	-1	0	29.22	-1	-1	0	36.41
2	1	-1	0	27.88	1	-1	0	36.96
3	-1	1	0	34.94	-1	1	0	42.25
4	1	1	0	38.85	1	1	0	42.33
5	-1	0	-1	29.15	-1	0	-1	32.76
6	1	0	-1	34.26	1	0	-1	37.86
7	-1	0	1	33.3	-1	0	1	38.91
8	1	0	1	36.87	1	0	1	38.43
9	0	-1	-1	28.2	0	-1	-1	30.62
10	0	1	-1	35.24	0	1	-1	38.69
11	0	-1	1	29.71	0	-1	1	37.21

Table 6
(continuation)

No.	Seed test design and results				Powder test design and results			
	C_m	D_m	G_m	Angle of repose (°)	B_s	C_s	G_s	Angle of repose (°)
12	0	1	1	40.53	0	1	1	39.96
13	0	0	0	39.64	0	0	0	40.55
14	0	0	0	39.95	0	0	0	41.17
15	0	0	0	41.77	0	0	0	41.53
16	0	0	0	41.1	0	0	0	41.31
17	0	0	0	39.82	0	0	0	41.7

Table 7

Analysis of variance for Box-Behnken test results

Analysis of variance for seed test results					Analysis of variance for powder test results				
Source of variance	Mean square	Degree of freedom	Sum of squares	P-value	Source of variance	Mean square	Degree of freedom	Sum of squares	P-value
Model	43.02	9	387.22	<0.0001**	Model	18.85	9	169.61	<0.0001**
C_m	15.82	1	15.82	0.0082**	B_s	3.45	1	3.45	0.0244*
D_m	149.21	1	149.21	<0.0001**	C_s	60.67	1	60.67	<0.0001**
G_m	22.98	1	22.98	0.0032**	G_s	26.57	1	26.57	<0.0001**
$C_m D_m$	6.89	1	6.89	0.0468*	$B_s C_s$	0.0552	1	0.0552	0.7281
$C_m G_m$	0.5929	1	0.5929	0.5025	$B_s G_s$	7.78	1	7.78	0.0036**
$D_m G_m$	3.57	1	3.57	0.1263	$C_s G_s$	7.08	1	7.08	0.0046**
C_m^2	63.36	1	63.36	0.0002**	B_s^2	2.05	1	2.05	0.0634
D_m^2	62.55	1	62.55	0.0002**	C_s^2	4.80	1	4.80	0.0119*
G_m^2	42.63	1	42.63	0.0005**	G_s^2	53.51	1	53.51	<0.0001**
Residual	1.19	7	8.31		Residual	0.4218	7	2.95	
Lack of Fit	1.61	3	4.84	0.2770	Lack of Fit	0.7238	3	2.17	0.1190
Pure Error	0.8669	4	3.47		Pure Error	0.1952	4	0.7809	
Cor Total		16	395.52		Cor Total		16	172.56	

$$\theta_1 = 40.46 + 1.41C_m + 4.32C_m + 1.31C_m D_m - 0.385C_m G_m + 0.945D_m G_m - 3.88C_m^2 - 3.85D_m^2 - 3.18G_m^2 \quad (7)$$

$$\theta_2 = 41.25 + 0.66B_s + 2.75C_s + 1.82G_s - 0.118B_s C_s - 1.4B_s G_s - 1.33C_s G_s - 0.7B_s^2 - 1.07C_s^2 - 3.56G_s^2 \quad (8)$$

The results of the Box-Behnken test ANOVA (analysis of variance) are shown in Table 7. Perform the ANOVA on the test results of the seeds, where C_m , D_m , G_m , C_m^2 , D_m^2 , and G_m^2 all have highly crucial effects on the rest angle; $C_m D_m$ has a significant effect on the angle of repose; the remaining parameters have no marked effect on the rest angle of the seeds. Conduct the ANOVA on the powder test results, where C_s , G_s , $B_s G_s$, $C_s G_s$, and G_s^2 had an extremely significant effect on the rest angle; B_s and C_s^2 have substantial effects on the rest angle of powder; the other parameters have no significant influence on the angle of repose of the powder. The p-values of the quadratic regression models for both seeds and powders are less than 0.001, where the seed regression model coefficient of determination $R^2 = 0.9790$ and Adjusted $R^2 = 0.9520$ are both close to 1 and with a coefficient of variation C.V. = 3.08%; powder regression model coefficient of determination $R^2 = 0.9829$ and Adjusted $R^2 = 0.9609$ are both close to 1 and the coefficient of variation C.V. = 1.68%. The results showed that the regression models for both seeds and powders are highly significant and could be used to analyse the angle of repose.

Optimization of the second-order regression equation is made to obtain the optimal combination of contact parameters for seeds and powders, using the rest angle of the physical test as the target value by Design-Expert 11.0 software: the inter-seed collision recovery coefficient is 0.188, the inter-seed static friction coefficient is 0.684, the static friction coefficient between seed and steel plate is 0.371; the inter-powder static friction coefficient is 0.887, the inter-powder rolling friction coefficient is 0.319, and the JKR surface energy is 0.162.

In order to verify the accuracy and reliability of the simulation calibration, the above parameters are used as the EDEM simulation parameters to simulate the angle of repose of seeds and powders, and the average rest angle of seeds is 32.81°, with a relative error of 0.21% compared with the physical test value of 32.74°; the average rest angle of powders is 41.28°, with a relative error of 0.983% compared with the physical test value of 41.69°. The test results indicate no significant difference between the simulated rest angle and the rest angle of the physical test, and the experimental comparison is shown in Figure 7.

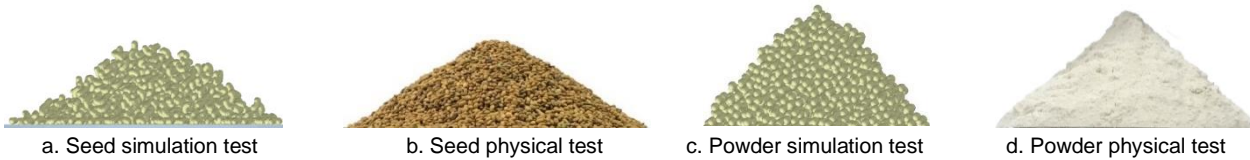


Fig. 7- The angle of repose test comparison

Simulation test of restitution coefficient between powder and seed

The static friction coefficient a_2 and rolling friction coefficient a_3 between seed and powder, the collision recovery coefficient a_4 , static friction coefficient a_5 and rolling friction coefficient a_6 between powders do not affect the seed rebound height; set them to 0 for the simulation. Take the range of collision recovery coefficient of seed and powder a_1 as 0.1~0.3, set the step size as 0.05 for 6 sets of tests, get the seed to rebound height b_1 , the simulation test model is shown in Figure 8, the test design and results are shown in Table 8, the fitting equation is shown in Eq.9. The rebound height of 8.01 mm measured in the physical test is brought into the equation and solved for a_1 of 0.246, and the results are input into EDEM for simulation test, and the rebound height is 8.07 with a relative error of 0.75%.

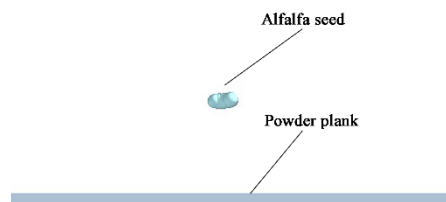


Fig. 8- Collision recovery coefficient simulation test

Table 8

Simulation test design and results

No.	a_1	b_1/mm
1	0.1	2.499
2	0.15	4.615
3	0.2	6.09
4	0.25	8.502
5	0.3	9.809
6	0.35	13.39

$$b_1 = 20.01479a_1 + 47.52143a_1^2 + 0.22856 \tag{9}$$

Simulation test of the static friction coefficient between powder and seed

Set the calibrated collision recovery coefficient a_1 of seed and powder to 0.246, set a_3, a_4, a_5 and a_6 to 0, the range of static friction coefficient between seed and powder a_2 is taken as 0.6~0.85, set the step size as 0.02 for 6 sets of tests, obtain the rotation angle b_2 of the inclinometer, the simulation model is shown in Figure 9 the test design and results are shown in Table 9, the fitting equation is shown in Eq.10. The angle of rotation of the inclinometer 31.85° measured by the physical test is brought into the equation and solved for a_2 of 0.776, and the simulation test is averaged to obtain the angle of rotation of the inclinometer of 32.06° with a relative error of 0.66%.

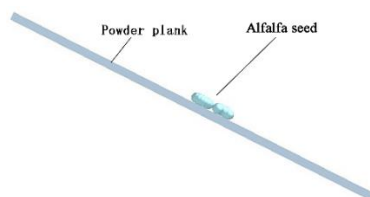


Fig. 9 - Static friction coefficient simulation test

Table 9

Simulation test design and results

No.	a_2	b_2/mm
1	0.7	20.4
2	0.72	22.86
3	0.74	24.12
4	0.76	29.04
5	0.78	32.76
6	0.8	37.8

$$b_2 = -1349.025a_2 + 015.17857a_2^2 + 467.37643 \quad (10)$$

Simulation test of the rolling friction coefficient between powder and seed

Set the collision recovery coefficient a_1 to 0.246, set the static friction coefficient a_2 to 0.776; a_4 , a_5 and a_6 are all set to 0. The seed and powder rolling friction coefficient a_3 are taken to range from 0.2 to 0.3, set the step size as 0.02 for 6 sets of simulation tests. b_3 is the horizontal rolling distance of alfalfa seeds, and the simulation model is shown in Figure 10. The test design and results are shown in Table 10, and the fitting equation is shown in Eq.11. Bring the horizontal rolling distance $b_3 = 69.2$ measured by the physical experiment into the equation, and solve for a_3 of 0.255. Conduct the simulation test, the horizontal rolling distance of the seed is 68.74 mm, and the relative error is 0.66%.



Fig. 10- Rolling friction coefficient simulation test

Table 10

Simulation test design and results

No.	a_3	b_3/mm
1	0.2	114.6
2	0.22	93.12
3	0.24	81.51
4	0.26	63.08
5	0.28	56
6	0.3	39.88

$$b_3 = -1721.80714a_3 + 2005.35714a_3^2 + 377.47571 \quad (11)$$

CONCLUSIONS

By physically determining the basic physical and contact parameters of seeds and powders, a series of simulation tests were conducted based on particle scaling theory and particle contact theory using EDEM, and the response surface analysis was performed on the simulation results to obtain the best combination of contact parameters for discrete element simulation of seeds and powders; the comparison test results showed that there is no significant difference between the simulation test and physical test results, which verified the accuracy of the simulation parameter combination. It was found that according to the characteristics of different materials, using different contact models for simulation tests could precisely simulate the movement characteristics of materials in actual production; in addition, the calibration of contact parameters in this study has particular reference significance for the follow-up study of similar fine seeds and powder materials.

ACKNOWLEDGEMENTS

We acknowledge that this work was supported by the National Natural Science Foundation of China under the project "Research on structural parameters of split-flow hedge sand collector and its internal flow field characteristics (41661058)", the Natural Science Foundation of Inner Mongolia Autonomous Region under the project "Research on the working parameters of grass seed pill granulation coating and its coating mechanism under the action of the vibration force field (2018MS05023)" and the project "Program for improving the Scientific Research Ability of Youth Teachers of Inner Mongolia Agricultural University".

REFERENCES

- [1] Afzal, I., Javed, T., Amirkhani, M., (2020), Modern seed technology: seed coating delivery systems for enhancing seed and crop performance. *Agriculture*, 10;
- [2] Favier, J. F., (2001), Modelling nonspherical particles using multisphere discrete elements. *Journal of Engineering Mechanics*, 127(10), 971-977;
- [3] Gui Z., Babaimin A., Gulibahar T., Kanzha & Wang, Z.. (2018). DEM method to analyse the effect of drum inner wall structure on mixing behaviour. *Feed Industry* (21), 5-9;
- [4] Hou Z., Dai N., Chen Z., (2020), Determination of physical parameters of ice grass seeds and calibration of discrete element simulation parameters. *Journal of Agricultural Engineering* (24), 46-54;
- [5] Horabik, J., Beczek, M., Mazur, R., Parafiniuk, P., & Molenda, M.. (2017), Determination of the restitution coefficient of seeds and coefficients of visco-elastic hertz contact models for DEM simulations [J]. *Biosystems Engineering*, 161, 106-119;
- [6] Liu F., Zhang J., Li B., & Chen J.. (2016). Analysis and calibration of discrete element parameters for wheat based on stacking tests [J]. *Journal of Agricultural Engineering* (12), 247-253;
- [7] Liu W., He J., Li H., (2018), Simulation parameter calibration of mini-potato based on discrete element[J]. *Transactions of the Chinese Society of Agricultural Machinery*, 49(05): 125-135+142;
- [8] Markauskas D., Ramírez-Gómez Á., Kačianauskasa R., Zdancevičius E., (2015), Maize grain shape approaches for DEM modelling. *Computers and Electronics in Agriculture*, vol.118, pp.247-258;
- [9] Pachón-Morales J., Do H., Colin J., Puel F., (2019), DEM modelling for flow of cohesive lignocellulosic biomass powders: model calibration using bulk tests. *Advanced Powder Technology*;
- [10] Peng C., Xu D., He X., Tang Y., & Sun S..(2020), Parameter calibration of the discrete element simulation model for pig manure organic fertilizer treated by Heishui Fly[J]. *Transactions of the Chinese Society of Agricultural Engineering*, 36(17): 212-218;
- [11] Ren J., Zhou L., Han L., Zhou J., & Yan M.. (2017), Discrete simulation of vertical spiral conveying based on particle scaling theory [J]. *The Chinese Journal of Process Engineering*, 17(05): 936-943;
- [12] Shi L., Zhao W., & Sun W.. (2017), Discrete element-based farmland soil particle contact model and parameter calibration in the arid area of Northwest China [J]. *Transactions of the Chinese Society of Agricultural Engineering*, 33(21):181-187;
- [13] Subhash C., Thakur., Jin Y., & Hossein A..(2016). Scaling of discrete element model parameters for cohesionless and cohesive solid. *Powder Technology*;
- [14] Wu T., Huang W., Chen X., Ma X., Han Z., & Pan T.. (2017), Discrete element model parameter calibration of cohesive soil considering the cohesion between particles [J]. *Journal of South China Agricultural University*, 38(03): 93- 98;
- [15] Zhang L., Wang H., Guo Y., Li S., & Wang F.. (2020), Blueberry Discrete Element Parameter Calibration Based on Response Surface Method[J]. *Journal of Shenyang Agricultural University*, 51(05): 540-548;
- [16] Zhao M., (2015), *Research on the sieving characteristics of alfalfa seeds and its control system optimization design of cleaning equipment* (Doctoral dissertation, China Agricultural University);
- [17] Zhou, L.. (2017), *EDEM simulation and experimental study of vertical screw conveying* (Master's thesis, Zhejiang University of Technology);
- [18] Zeng Z., Ma X., (2021), Critical Review of Applications of Discrete Element Method in Agricultural Engineering [J]. *Transactions of the Chinese Society of Agricultural Machinery*, 52(04):1-20.